Carrier Phase DGPS for Autonomous Airborne Refueling

Samer Khanafseh and Boris Pervan, *Illinois Institute of Technology*, Chicago, IL
Glenn Colby, *Naval Air Warfare Center*, Patuxent River, MD

ABSTRACT

For Autonomous Airborne Refueling (AAR) to be possible, the position of the receiving aircraft relative to the tanker must be known very accurately in real time. In addition, to ensure safety and operational usefulness, the navigation architecture must also provide high levels of integrity, continuity, and availability. In this paper, we begin with the latest proposed Shipboard Relative GPS (SRGPS) navigation architecture, which uses Carrier Phase DGPS (CDGPS), and we exploit it as a preliminary basis for AAR navigation. However, the AAR mission is somewhat different from SRGPS because of the potentially severe sky blockage introduced by the tanker. Blockage models are presented and preliminary availability analyses for AAR are carried out using the SRGPS-derived navigation processing architecture. In this work, we analyze the AAR navigation problem, quantify system availability using SRGPS algorithms and investigate the benefits of ranging augmentation. Sensitivity analyses of availability with respect to different architecture elements and parameters are then performed. Finally, the analytical tools developed throughout this work were used to plan the AAR flight tests. The GPS and INS data collected were evaluated with offline GPS algorithms and used to validate the sky blockage model and simulations.

INTRODUCTION

Unmanned Air Vehicles (UAVs) have recently generated great interest because of their potential to perform hazardous missions without endangering the lives of pilots and crews. In order to extend the mission range of these vehicles, it has been proposed that they should be refuelable *in-air* using currently available tanker aircrafts. Since UAVs are unmanned, these refueling missions must take place autonomously. For this to be possible, the position of the UAV relative to the tanker must be known very accurately in real time. In addition, to ensure safety and operational usefulness, the navigation architecture must also provide high levels of integrity, continuity, and availability. Overall the navigation requirements for autonomous air refueling (AAR) are similar to those for the shipboard landing of aircraft. In this paper, we begin with the latest proposed Shipboard Relative GPS (SRGPS) navigation architecture [1], which uses Carrier Phase DGPS (CDGPS), and we exploit it as a preliminary basis for AAR navigation. However, the AAR mission is somewhat different from SRGPS because of the potentially severe sky blockage introduced by the tanker in AAR. Therefore, we analyze the AAR navigation problem, quantify system availability using SRGPS algorithms, and investigate the benefits of ranging augmentation.

The latest proposed SRGPS algorithms provide robust CDGPS performance by combining the complementary benefits of geometry-free filtering and geometric redundancy. Specifically, when the UAV is far from the tanker, inside or outside the service volume (i.e., the region where tanker reference GPS measurements are available to the UAV), geometry-free filtering is used for cycle estimation of widelane integers. For dual frequency implementations, the advantage of code/carrier divergence-free filtering prior to the service volume entry can be especially significant because long filter durations can be used. The use of geometric redundancy for cycle resolution is restricted to the service volume, where the UAV has access to the tanker reference measurements, and is more robust to ionospheric and tropospheric decorrelation because the distance between the UAV and the tanker is small. Therefore, only when the UAV is near the tanker, can carrier phase geometric-redundancy be safely exploited for cycle estimation of any remaining widelane integers and, if needed, L1 and L2 integers. However, from the point of view of terminal navigation, the primary difference between SRGPS and AAR is sky blockage from the tanker.

There are two main types of in-flight refueling systems currently in use: the *drogue* system which most U.S. Navy aircraft use and the *boom* system which the U.S. Air Force uses. In the drogue system, a hose with a cone-shaped basket at the end is winched out from the tanker with (Figure 1-a). The receiving aircraft has a probe, which the pilot guides into the basket. The boom system,

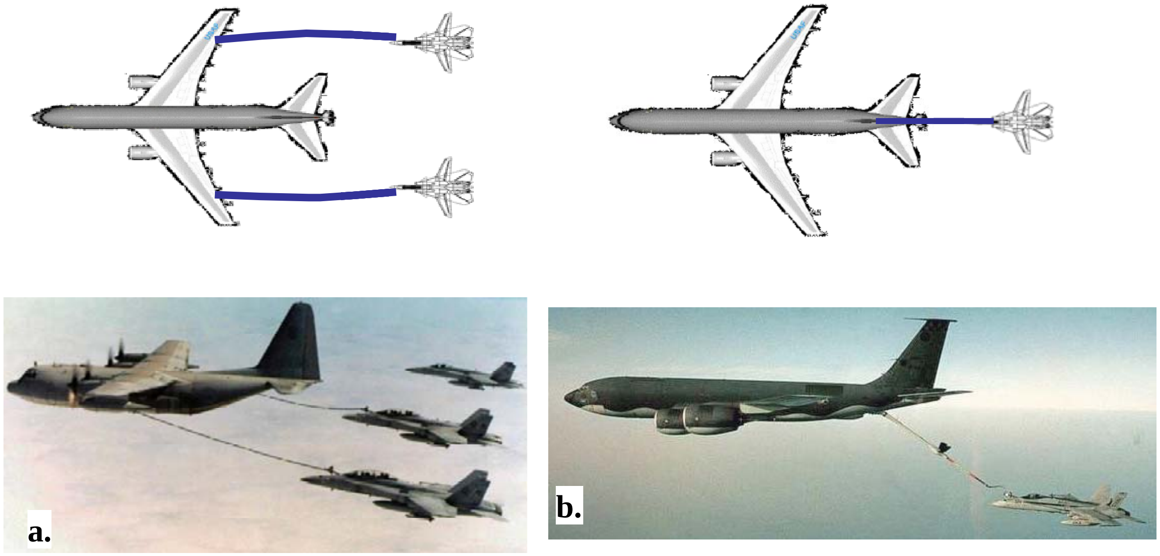

Figure 1: Air Refueling Systems. a) Drogue System and b) Boom System

in contrast, has a fixed boom which is lowered from the tanker, and its end is extended into a socket on the top of the receiving aircraft (Figure 1-b). Today, there are three types of tanker airplanes used for in-flight air refueling: KC-135, KC-10 and KC-130. If the drogue system is used with the KC-10 and KC-130, the sky blockage caused by the tanker aircraft is relatively small because the drogue hose is winched from the wings of the airplane (Figure 1-a). However, the KC-135 is a larger aircraft and therefore causes much greater sky masking, especially when implemented with a boom system.

In this work, the boom system is studied because it causes larger sky blockages than the drogue system. Blockage models are presented and preliminary availability analyses for AAR are carried out using the SRGPS-derived navigation processing architecture. Sensitivity analyses of availability with respect to different architecture elements and parameters are then performed. Next, the analytical tools developed throughout this work were used to plan the AAR flight tests that took place in September 2004. Finally, the GPS and INS data collected during these trials were used to validate the sky blockage model and simulations.

AVAILABILITY ANALYSIS

In this work, *availability* is defined as the percentage of time under which the Vertical Protection Level (VPL) is smaller than a Vertical Alert Limit (VAL) of 1.1 m. The VPL is a function of the integrity risk (10^{-7} for SRGPS), the satellite geometry, and precision of GPS measurements. The VPL is generated by covariance analysis of the proposed SRGPS architecture. The processing starts by prefiltering narrow-lane code against widelane carrier in both the tanker and receiver aircraft. In this analysis, a maximum prefiltering period of 30 minutes is assumed to generate floating estimates of the widelane cycle ambiguities. When the receiver aircraft is close to the tanker, the broadcasted floating widelane ambiguities from the tanker are combined with the receiver aircraft floating ambiguities. Geometric redundancy is exploited to fix those widelane and L1 and L2 integers which meet a 10^{-8} constraint for probability of incorrect fix. The geometric redundancy process is facilitated by LAMBDA decorrelation [4]. (In subsequent sensitivity analyses the integrity risk requirement was relaxed to 10^{-4}, and the associated cycle resolution risk threshold to 10^{-5}.) After the integer fixing process, the position of the receiver aircraft can be estimated. The vertical component of the position estimation standard deviation (σ_V) is calculated and used to generate VPL. VPL was calculated by multiplying σ_V by the integrity risk multiplier corresponding to the integrity risk requirement (5.33 in the case of 10^{-7} integrity risk).

Using different values of code and carrier 'sigmas' (single difference standard deviations), the service availability without blockage is calculated and shown in Figure 2. These results (and those that follow) assume a first order Gauss-Markov measurement error model with a time constant of one minute. In the service availability simulations, the effect of depleted GPS satellite constellations is also included using the 'minimum standard' constellation state probability model provided in the GPS Service Performance Standard (GPS SPS) [2]. Given the same VAL requirements, AAR service availability is expected to be lower because of the shadowing caused by the tanker airplane. Therefore, before calculating the AAR availability, a satellite blockage model must be established.

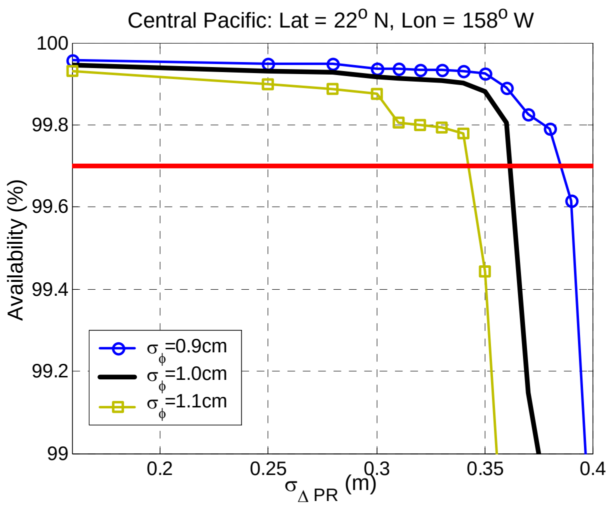

Figure 2: Availability without Sky Blockage at Central Pacific for Different Code and Carrier Sigmas.

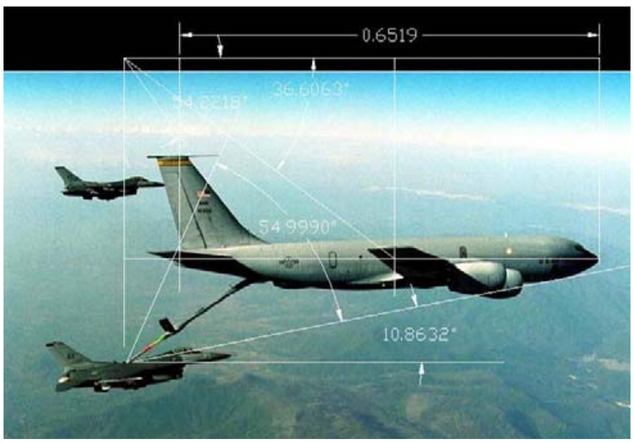

Figure 3: Reverse Engineering to Determine the Masking Wedge Geometry of KC-135

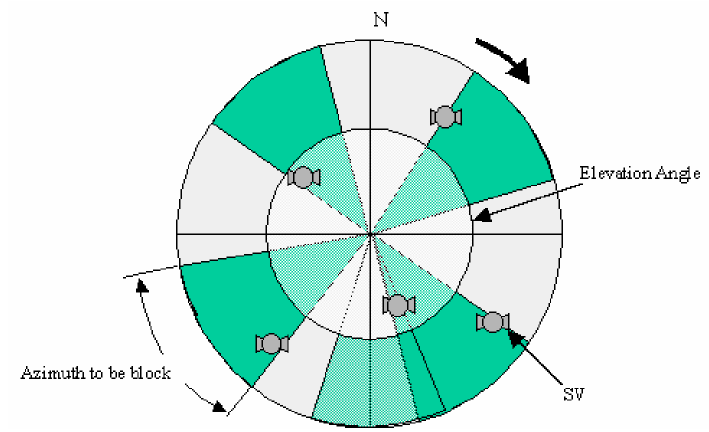

Figure 4: Schematic Diagram Showing the Method Used to Determine the Worst VDOP

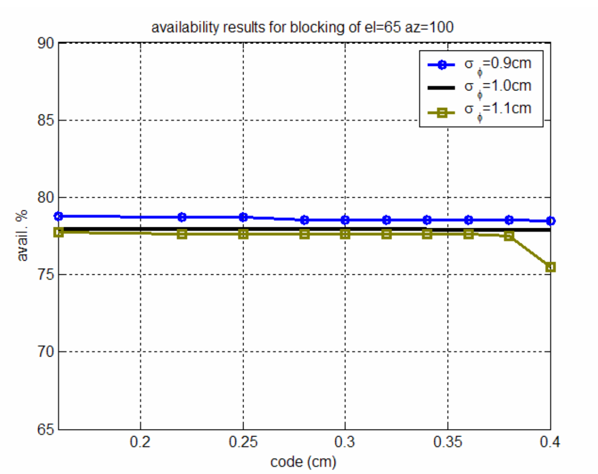

Figure 5: AAR Service Availability at Central Pacific Using KC-135 Wedge Model

AAR AVAILABILITY USING A SIMPLE BLOCKAGE MODEL

A preliminary blockage model was created by "reverse engineering" masking geometries from photographs. Pictures of the KC-135 tanker from different views were used to calculate the azimuth and elevation of the masking-wedge that the tanker shadows from the sky (Figure 3). The service availability is calculated based on the worst-case azimuth orientation of the tanker flight path at each sampled time during the day. (VDOP is used as the metric to define the worst case.) To determine the worst case orientation for a given satellite geometry, it is not necessary to apply the azimuth-elevation mask to all possible orientations. Only the azimuths at which satellites are located need to be considered. Initially, the wedge is aligned with one of the satellites in view and all the satellites that fall in the masked region are eliminated from the constellation (Figure 4). By rotating the wedge to be aligned with each of the satellites, the worst possible case (VDOP) is guaranteed to be captured. This method produces the same results as if all possible orientations are tested, but it is much more time efficient.

For the KC-135, the masking wedge size was approximated to be 65 deg in elevation and 100 deg in azimuth. A nominal 7.5 deg elevation mask was used outside the wedge. The availability results are shown in Figure 5. The results show that when the KC-135 blockage wedge-mask is applied to the architecture, the availability drops from 99.9% to 77%. It is immediately clear that terminal navigation availability is highly sensitive to sky blockage. As discussed below, for other (smaller) tanker aircraft, the availability results will be somewhat better. Recall also that the SRGPS requirements were used here, and the availability performance will change if AAR requirements are different. In the next section, the sensitivity of availability to different wedge sizes (wedge azimuth and elevation values), nominal elevation mask, and integrity risk will be quantified.

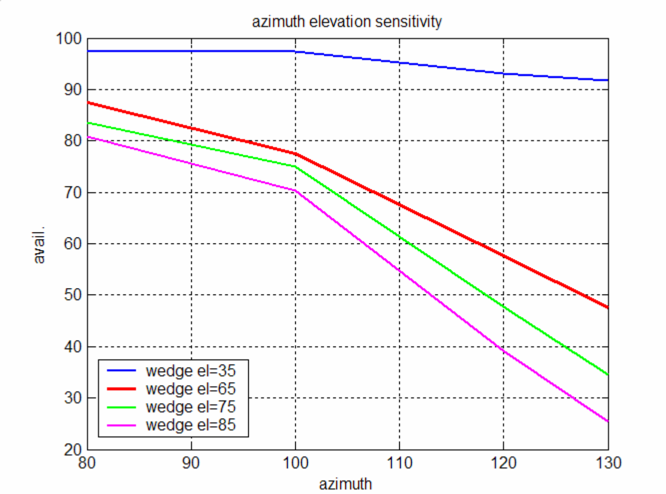

Figure 6: Service Availability at Central Pacific as a Function of Wedge Azimuth and Elevation

Table 1: Navigation Availability Sensitivity to other Parameters.

Sensitivity parameter	parameter value	Availability %
Nominal	NA	77.5
Integrity risk	$1x10^{-4}$	79.9
low elevation mask	3 deg.	95.2
LAL	1.1 m	79.2

SERVICE AVAILABILITY SENSITIVITY ANALYSIS

For different tanker airplanes, like the KC-10 and KC-130, the same method of reverse engineering could not be used to determine the wedge angles because of a lack of suitable images of these aircraft during refueling. Instead, a range of masks with different azimuth and elevation angles were used to span the different possible combinations of tankers, fighters and refueling systems. The azimuth values used were 80, 100, 120 and 130 deg and the elevation angles were 35, 65, 75 and 85 deg. Availability simulations were performed using all combinations of these wedge angle values. Figure 6 shows the availability at different wedge azimuth and elevation masks. It can be seen, for example, that the availability is reduced from 88% to 48% as the wedge azimuth increases from 80 to 130 degrees while holding elevation mask at 65 degrees. For the wedge sizes considered, the service availability ranges from 27% to 98%. Because of this extreme sensitivity to the blockage, it is clear that a much more accurate blockage model will be required to precisely define navigation availability. Such a model for the KC-135 will be described shortly.

Navigation availability sensitivity to other parameters, including the general elevation mask (outside the wedge), the integrity risk requirement, and use of the Lateral Alert Limit (LAL) instead of the VAL, was also quantified. The results are shown in Table 1 for the KC-135 wedge, sigma code of 30 cm and 1.0 cm sigma carrier. Since air refueling missions are conducted at high altitudes, the elevation mask outside the wedge can probably be safely lowered from 7.5 to 3 degrees. The resulting availability is significantly improved to 95.2%. In contrast, relaxing the integrity risk requirement from 10^{-7} to 10^{-4} (and also the cycle resolution probability of correct fix requirement from 10^{-8} to 10^{-5}) improved the availability by 2%. Finally, it is also shown in Table 1 that LAL availability is higher than VAL availability, but only by about 2% for LAL = 1.1 m.

In summary, relaxing the integrity risk requirement from 10^{-7} to 10^{-4} or using LAL instead of VAL (but keeping the level at 1.1 m) has little impact on the average service availability. On the other hand, lowering the general elevation mask from 7.5 degrees to 3 degrees has a more significant effect. In addition, as will be discussed shortly, the average service availability can be significantly improved by the addition of a ranging source on the belly of the tanker. However, before we quantify the performance benefits of such an augmentation it is useful to reexamine the existing performance in terms of *operational* availability, which is characterized by outage durations and number of outages, rather than only the simple time fraction described by the service availability.

OPERATIONAL AVAILABILITY ANALYSIS

In this part of the analysis, satellite outage state probability models are no longer used, and we focus specifically on the KC-135 wedge model (65 deg elevation wedge mask and 100 deg azimuth) at central pacific and a single value of raw code standard deviation (30 cm) and carrier standard deviation (1 cm). Figure 7-a shows the VPL traces for 24 hour period and the VAL line at 1.1 m. Each point that lies above the red line (VAL limit) is called a "VPL_{H0} outage" to indicate that the positioning is either poor because of poor geometry or the number of visible satellites is less than four. The fraction of time without a VPL_{H0} outage in Figure 7-a is 79%, consistent with the prior service availability result of 77%, which incorporates a satellite outage model.

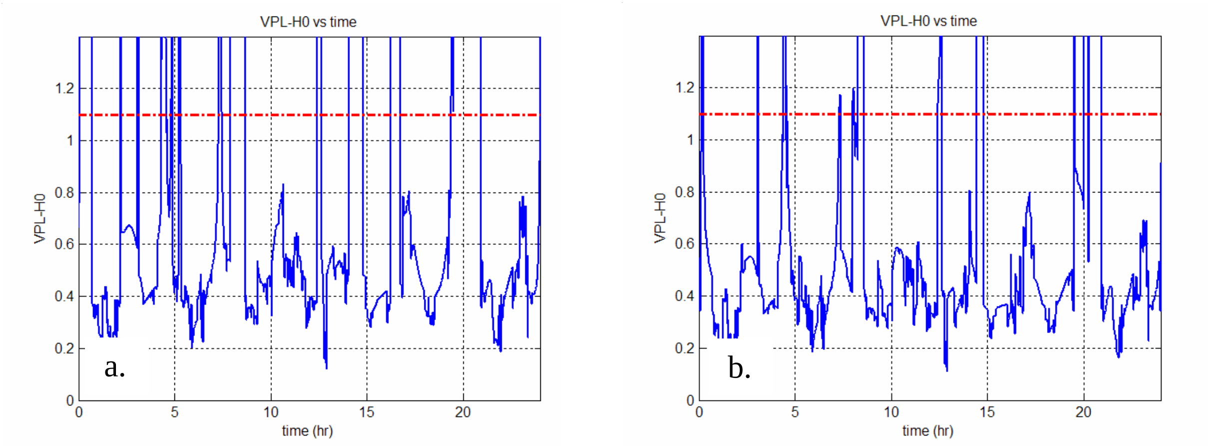

Figure 7: VPL Traces Over 24 Hours. a) without Ranging Augmentation, b) with TTNT Ranging Added

To evaluate the effect of ranging augmentation, we assume the existence of a Tactical Targeting Network Technology (TTNT) ranging signal originating at the belly of the KC-135 tanker (47 feet forward from the tail) and having a measurement ranging standard deviation of 15 cm. Although the assumed error standard deviation for the TTNT measurement is relatively high compared to GPS carrier phase, the addition of the measurement originating from the center of the blockage has significant impact on position quality. This is clearly shown in Figure 7-b, where the total time below VAL was raised from 79% to 91% after the addition of the TTNT ranging measurement.

The effects of the changes in the GPS satellite constellation and in the geographic location of the air refueling mission were also investigated. Results using the nominal 24 satellite constellation (used so far) were compared to the proposed 27 satellite constellation [3] (24 nominal (do229a) + 3 operational spares) at six different locations, which are marked in Figure 8 and detailed in Table 2. In this analysis, the VPL outages are shown as a function of flight azimuth (rather than the worst orientation only) in increments of 15 degrees. As shown in Figures 9 and 10, the availability results are sensitive to location but are clearly improved overall for the 27 satellite constellation.

DETAILED KC-135 BLOCKAGE MODEL

The previous results have shown that AAR terminal navigation availability is highly sensitive to the size of the sky blockage induced by the tanker. The wedge blockage model used in the initial analysis above, while simple and efficient, is very conservative because it covers areas in the sky that are not actually blocked by the tanker airplane. For this reason, a high fidelity blockage model was developed using 3-D CAD drawings of KC-135 obtained from Boeing (Figure 11-a).

Using the CAD drawings, three 2-D horizontal sections at different heights were extracted: one at the level of the horizontal tail stabilizers that captures the stabilizers, one at the level of the fuselage and engines to capture them, and one at the level of the wings. For each section, a Boolean matrix was constructed with one degree resolution in both azimuth and elevation. The rows and columns of this matrix represent the azimuth and elevation of the line of sight vector from the receiver. In this matrix, a 'one' is assigned to the row-column (azimuth-elevation) element if the line of sight vector is blocked by the tanker, and zeros are assigned elsewhere. A logical OR operation between the three matrices (corresponding to the three sections) is used to account for the entire tanker body. A sample plot that visually demonstrates the difference between the wedge blockage model and the new blockage model is shown in Figure 11-b. It is clear that the wedge blockage model exaggerates the amount of the sky that the tanker actually obstructs.

Table 2: The Coordinates of the Six Locations Used.

No.	Location	Lat (deg)	Lon (deg)
1	OK-USA	35	97 W
2	Persian Gulf	26	50 E
3	Okinawa	27	128 E
4	Diego Garcia	-12	97 E
5	Atlantic Ocean	55	52 W
6	Central Pacific	19	166 E

Figure 8: The Six Locations at which Availability was Computed.

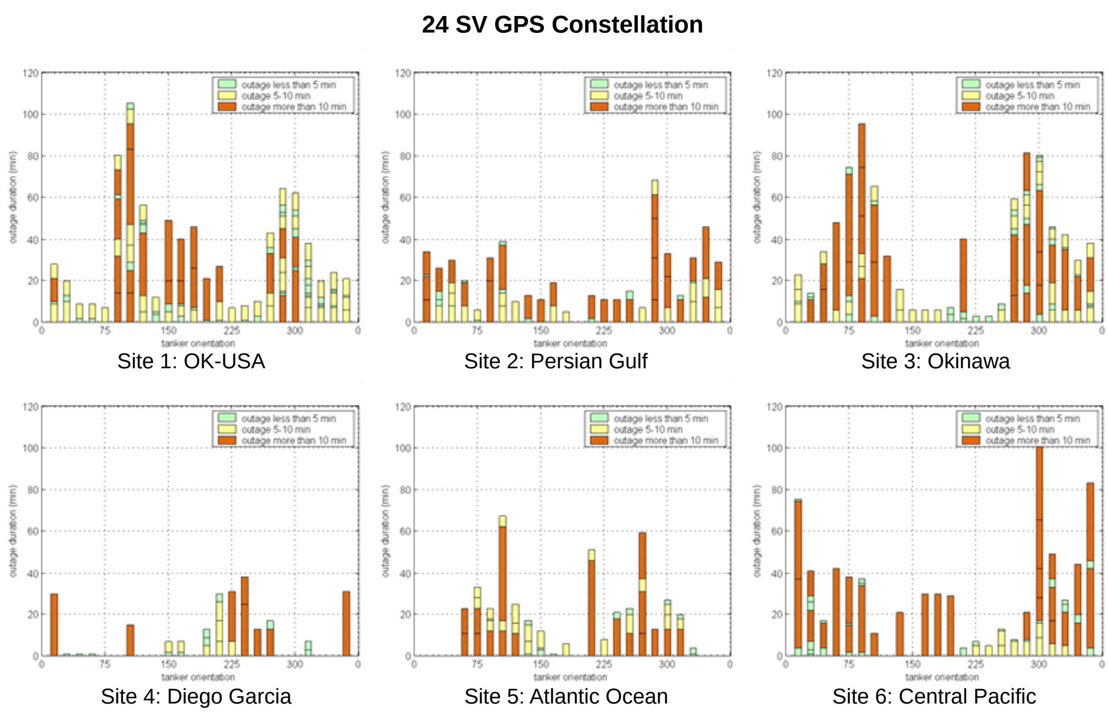

Figure 9: 24 Satellite Constellation VPL_{H0} Outages for the Six Locations

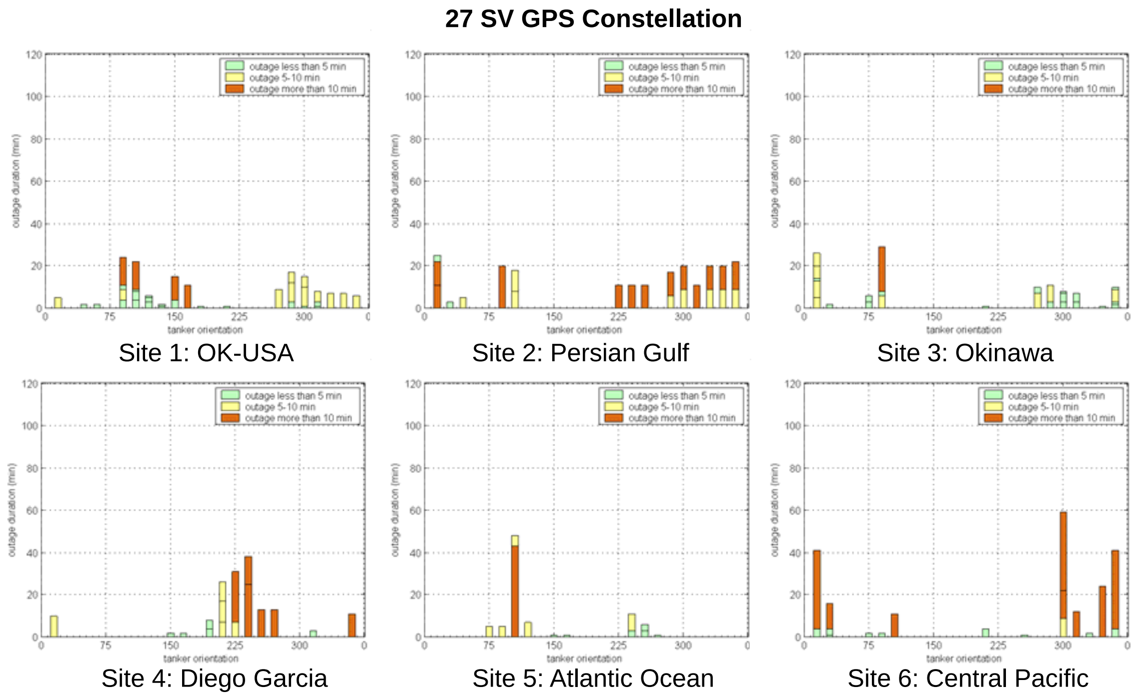

Figure 10: 27 Satellite Constellation VPL_{H0} Outages for the Six Locations

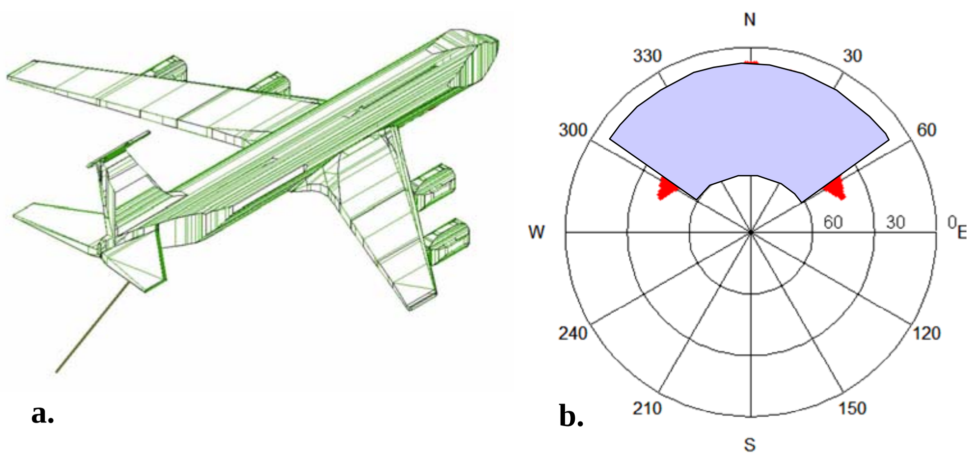

Figure 11: a) The CAD Drawing Used to Generate the Mask.
b) Polar Plot of the Sky Showing Old and New Blockage Models

Using the new blockage model, availability is calculated at different flight azimuth orientations in increments of 15 degrees. The effect of the new blockage model on availability has been tested by calculating the availability for the same six locations in Figure 8. The great improvement in availability obtained using the new blockage model can be seen by directly comparing the number and duration of VPL outages in using the wedge blockage model in Figure 10 to those using the new blockage model shown in Figure 12. In addition, the service availability for different code and carrier standard deviations is shown in Figure 13, where the service availability was also improved to 98%.

BLOCKAGE MODEL VALIDATION

AAR flight tests were planned to be conducted in September 2005 to obtain time-tagged GPS and INS data that will be evaluated with offline GPS algorithms and used to validate the sky blockage model and simulations.

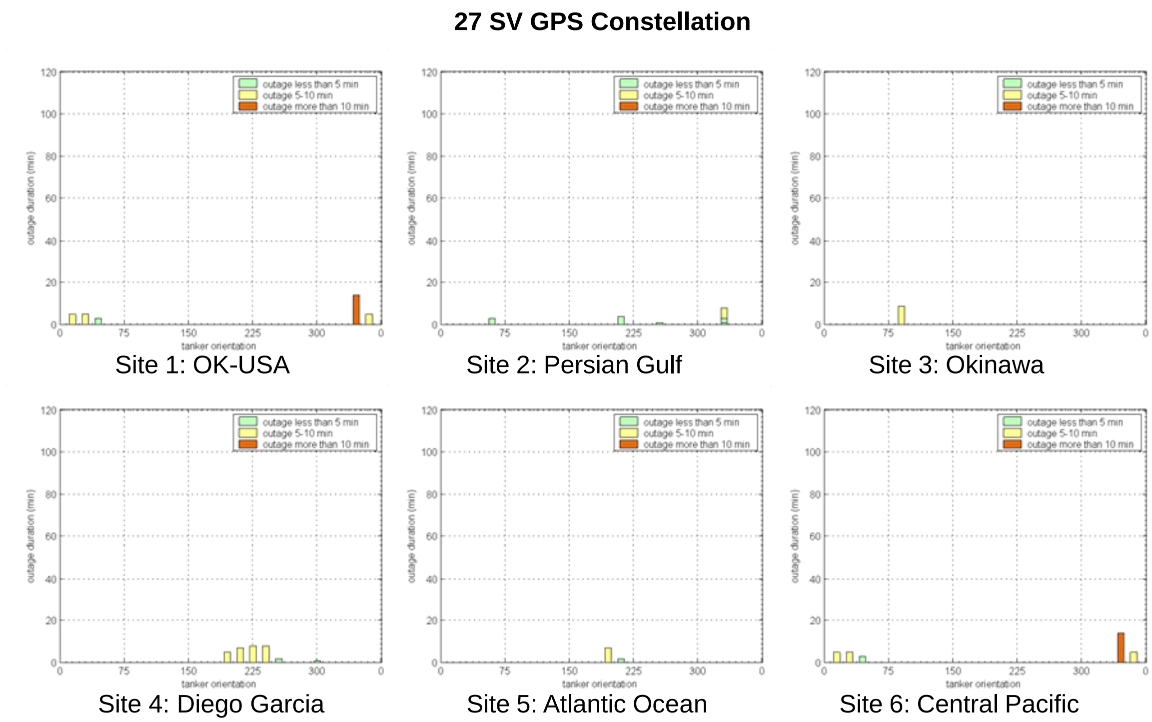

Figure 12: VPL$_{H0}$ Outages at Six Different Locations Using the New Blockage Model

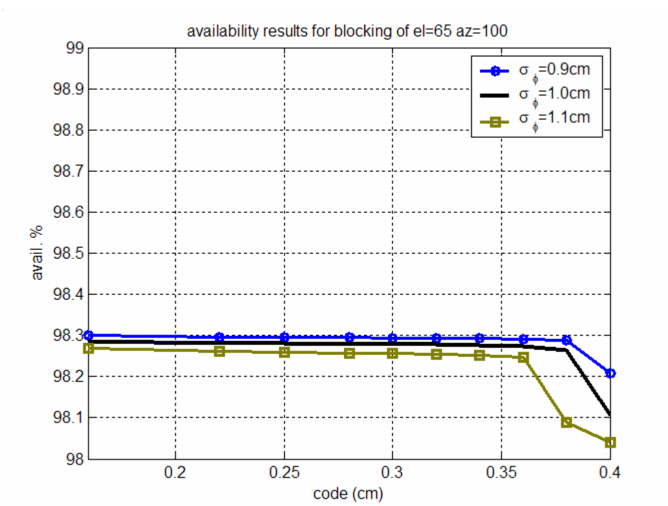

Figure 13: Service Availability at Central Pacific Using the New Blockage Model and (27) constellation

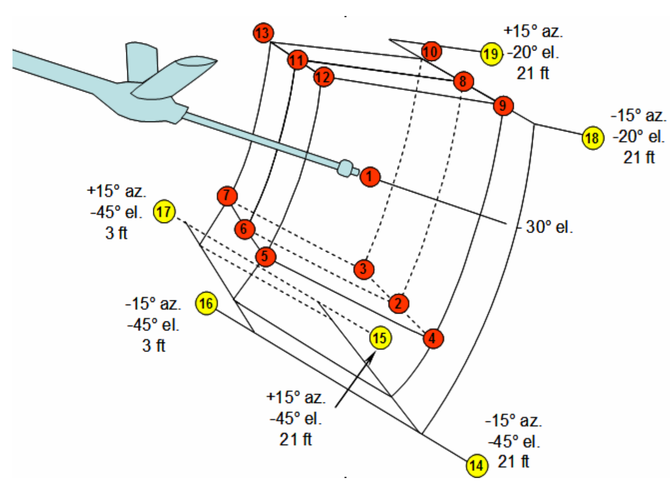

Figure 14: Different Test Point that Define the Refueling Envelope of the KC-135

To help in planning the flight tests, simulations were performed to define the flight times and azimuths that minimize GPS availability. The flight tests took place in Niagara Falls area (43 deg N, 97 deg W) during the second and third weeks of September 2004. In these simulations, almanac data from July 22, 2004 were used to provide predictions for a test date of September 15, 2004. The mission planning results were also applicable for other days during the flight test window by simply shifting outage events by four minutes per day. In these simulations, it was assumed that the standard deviations of GPS code and GPS carrier ranging measurement errors are 30 cm and 1 cm.

Nineteen different test point positions for the boom are used in the flight test to cover the KC-135R in-flight refueling envelope (Figure 14). In the mission planning process, these specified boom positions were used to generate a series of sky blockage matrices (one for each boom position). Using the sky blockage matrices, simulations for each of the boom points were conducted and the quantitative results for VPL_{H0} availability, VPL values, satellites in view, and sky blockage time traces were recorded. The resulting database is used to plan the flight test paths by flying in the direction and time slot for each test point when the satellite blockage or the satellite geometry is the worst. Samples of the plots that are used in preparing the flight test cards are shown in Figures 15 and Figure 16.

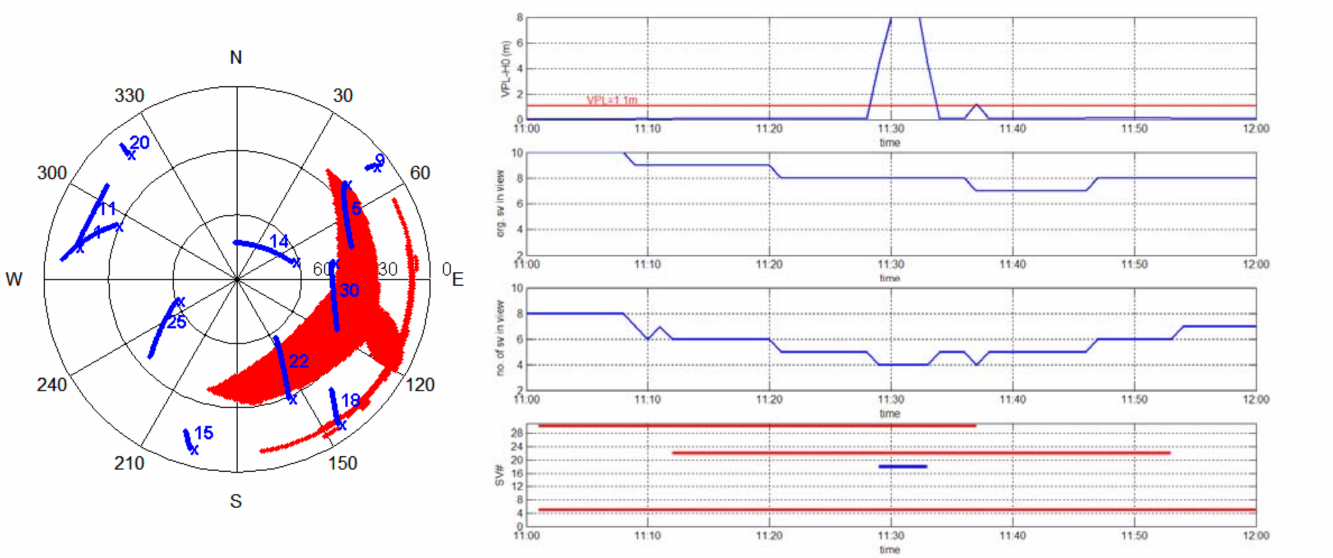

Figure 15: Samples of the Flight Test Simulation Results Used in Preparing the Flight Test Cards

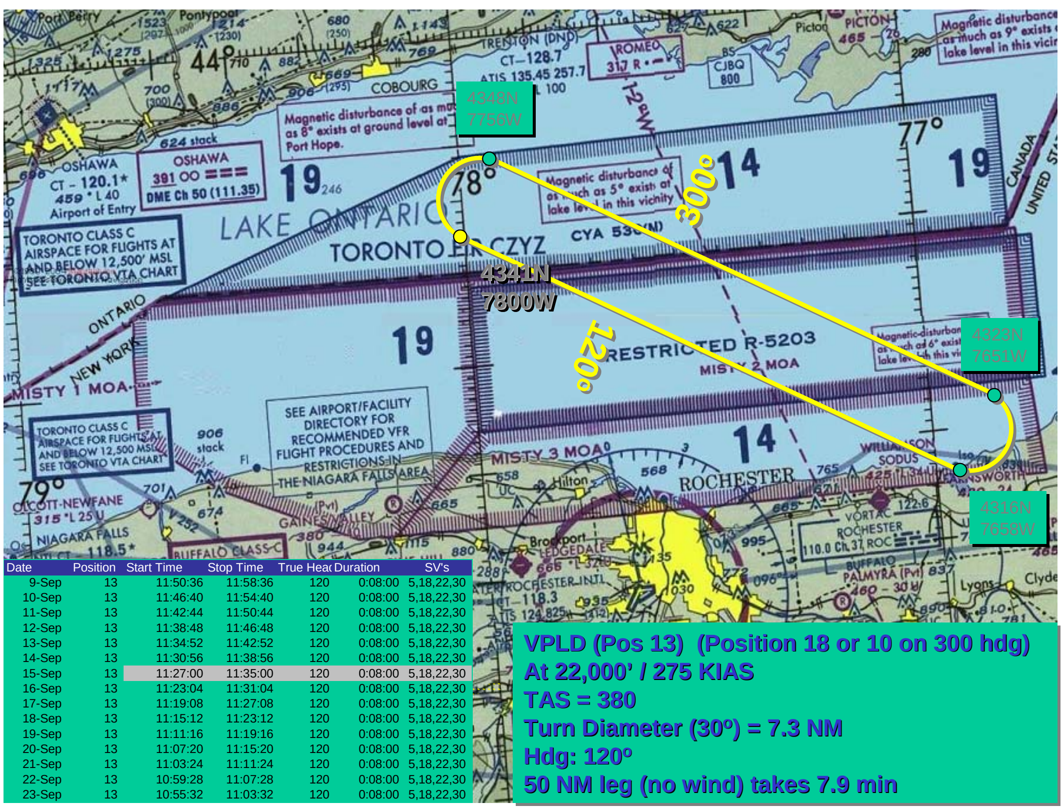

Date	Position	Start Time	Stop Time	True Head	Duration	SV's
9-Sep	13	11:50:36	11:58:36	120	0:08:00	5,18,22,30
10-Sep	13	11:46:40	11:54:40	120	0:08:00	5,18,22,30
11-Sep	13	11:42:44	11:50:44	120	0:08:00	5,18,22,30
12-Sep	13	11:38:48	11:46:48	120	0:08:00	5,18,22,30
13-Sep	13	11:34:52	11:42:52	120	0:08:00	5,18,22,30
14-Sep	13	11:30:56	11:38:56	120	0:08:00	5,18,22,30
15-Sep	13	11:27:00	11:35:00	120	0:08:00	5,18,22,30
16-Sep	13	11:23:04	11:31:04	120	0:08:00	5,18,22,30
17-Sep	13	11:19:08	11:27:08	120	0:08:00	5,18,22,30
18-Sep	13	11:15:12	11:23:12	120	0:08:00	5,18,22,30
19-Sep	13	11:11:16	11:19:16	120	0:08:00	5,18,22,30
20-Sep	13	11:07:20	11:15:20	120	0:08:00	5,18,22,30
21-Sep	13	11:03:24	11:11:24	120	0:08:00	5,18,22,30
22-Sep	13	10:59:28	11:07:28	120	0:08:00	5,18,22,30
23-Sep	13	10:55:32	11:03:32	120	0:08:00	5,18,22,30

Figure 16: A Sample of the Flight Test Cards Provided in the Mission

The collected data was post processed to validate the blockage model and the AAR algorithm architecture. In this paper, only the blockage model validation will be discussed. In previous simulations, the relative vector and the attitude of both aircraft were assumed to be static. However, to analyze the actual flight data, the fact that both aircrafts are moving continuously must be considered. Therefore, a new model that accounts for the dynamic changes was constructed. The dynamic model uses the relative position vector and the attitude information from both aircraft to create the tanker masking shadow and find the blocked satellites. The relative vector variations will change the location of the shadow in the UAV sky. In addition, the attitude of the tanker changes the orientation of the 2-D sections used in the detailed model. As a result, it will change the shape of the tanker shadow masking. On the other hand, the UAV attitude will not affect the shadow masking; instead, it will only change the low elevation mask for its antenna. This process is done at each epoch (5 sec. interval) during post-flight data analysis.

Figure 17 is a sample plot of the blockage model validation results. The number of satellites visible by the tanker and the UAV are shown in Figure 17-a and Figure 17-b respectively. The dynamic effect of the attitude and relative vector on the satellite blockage can be clearly seen in Figure 17-b. The movement of both aircraft causes the satellites to fall rapidly in and out of the tanker shadow which explains the trace shown in Figure 17-b.

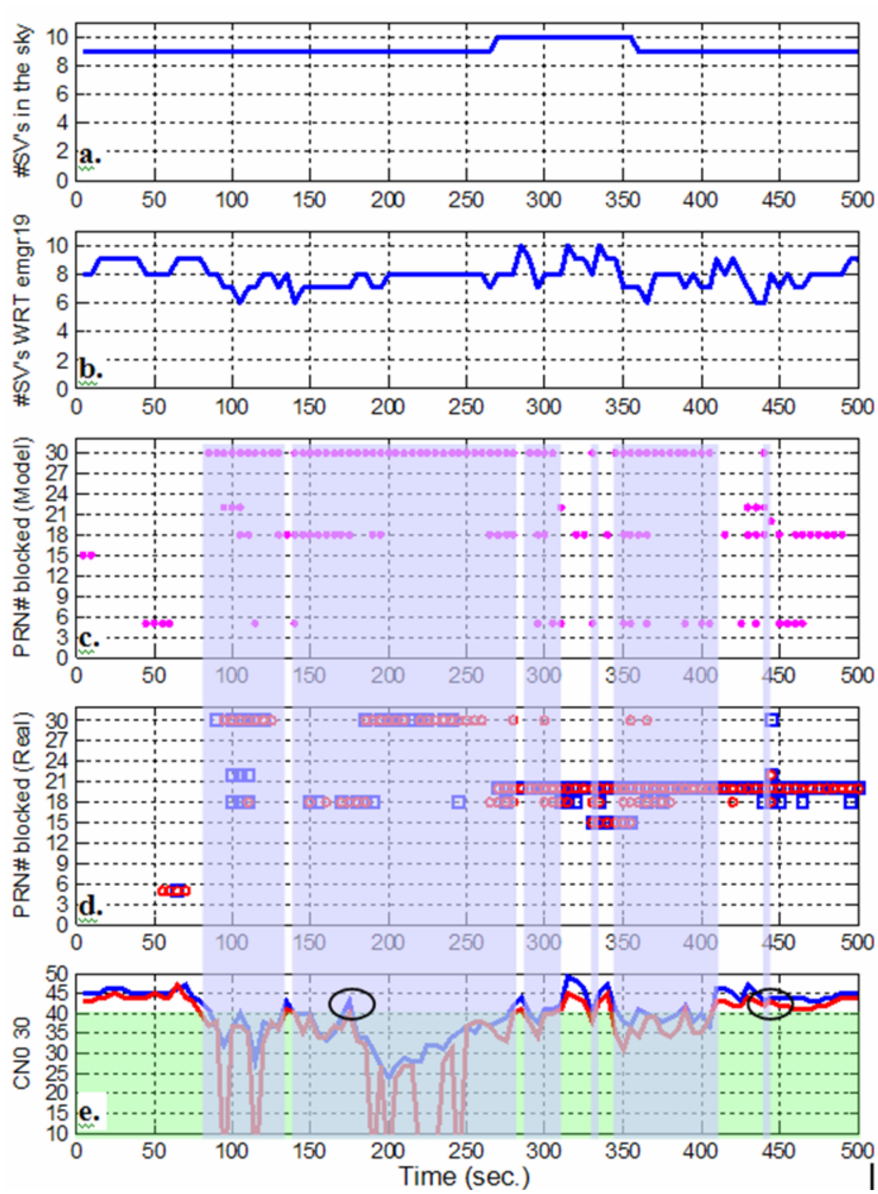

Figure 17: Blockage Model Validation Sample Plot. a) Number of Visible Satellites in the Tanker's Sky. b) Number of Visible Satellites in the Receiver's Sky. c) PRN number of the blocked satellites as predicted by the model. d) PRN number of the blocked satellites according to the measurements. e) C/N0 of PRN30.

The blocked PRNs as predicted by the model and as determined from the actual measurements are shown in Figure 17-c and Figure 17-d respectively. By comparing these two figures, it can be noticed that regarding the PRN numbers experiencing the outage, the model is consistent with the measurements. On the other hand, the model is more conservative in the sense that there are points that the model shows as blocked, while the phase lock is not lost in the measurements. To see if this is a defect in the model or not, C/N0 values for PRN30 were plot in Figure 17-e. In the case of a clear sky, C/N0 values were above 40dBHz which was chosen as a threshold. By comparing the times that PRN30 is blocked in Figure 17-c with the times when C/N0 values fall below 40dBHz it was found that they generally concur. The fact that when the model shows that PRN30 is blocked, C/N0 drops below 40dBHz mainly validates the blockage model described in this paper. However, some of the points in C/N0 do not match the model (marked in circles). These points can be explained by the approximations made in the blockage model. These approximations include neglecting the dihedral shape of the wings and stabilizers as well as neglecting the vertical tail. As a result, a new blockage model that utilizes the 3D shape of the tanker precisely is currently under development but not presented in this paper. In addition, by comparing the C/N0 values with the phase lock dropouts in the experimental data, it can be easily seen that there is inconsistency. If we neglect the current model flaws, the most probable interpretations will be that the signal gets weaker by penetrating the tanker body, but it stays strong enough to keep the lock or that the signal gets diffracted by the edges of the wings and stabilizers.

CONCLUSIONS

An SRGPS-based algorithm was used to evaluate terminal navigation performance for Autonomous Air Refueling. To make this algorithm applicable to AAR, sky blockage models were developed and were used to study the sensitivity of the availability to required integrity risk, elevation mask, flight azimuth orientation, and location. In addition, simulations of AAR flight test missions scheduled in September were performed and the results were used in the planning of these missions. The collected flight test data was post-processed to validate the simulations and the sky blockage model. Also, it will be used to assess the performance and applicability of the SRGPS-derived navigation architecture to AAR. In future work, navigation performance will be quantified as a function of TTNT ranging precision. The goal of these studies will be to establish derived requirements for TTNT ranging error. Finally, a more precise blockage model that utilizes the 3D shape of the tanker is currently under development.

REFERENCES

[1] M. Heo, B. Pervan, S. Pullen, J. Gautier, P. Enge, and D. Gebre-Egziabher, “Robust Airborne Navigation Algorithm for SRGPS,” *Proceeding of the IEEE Position, Location, and Navigation Symposium (PLANS '2004*), Monterey, CA, April 2004

[2] *Global Positioning System Standard Positioning Service Performance Standard*, October 2001.

[3] P. Massatt, F. Fritzen and M. Perz, “Assessment of the Proposed GPS 27-Satellite Constellation,” *ION GPS/GNSS 2003*, Portland, OR,September 2003

[4] P. Teunissen, D. Odijk, and P. Joosten, “A Probabilistic Evaluation of Correct GPS Ambiguity Resolution,” *Proceedings of the Tenth International Technical Meeting of the Satellite Division of the Institute of Navigation*, Nashville, TN, September 15-18, 1998.